The Effect of Manufacturing Variations on Unsteady Interaction in a Transonic Turbine

Dr. John Clark
Principal Engineer
AFRL/RQTT

16th Israeli Symposium on Jet Engines & Gas Turbines
Faculty of Aerospace Engineering
Technion, Haifa, Israel

09 November 2017

Approved for Public Release (88ABW-2017-5138)

Previous Investigations of Geometric Variability in Turbomachinery

Compressors

- Garzon and Darmofal, 2003: Effects on compressor performance
- Lange et al., 2011: Effects on stage performance
- Goodhand et al., 2012: Effects on incidence and 3D separations
- Schnell et al., 2013: Effects on fan performance, including unsteadiness
- Dow and Wang, 2015: Optimization of airfoils taking into account tolerances
- Reitz et al., 2016: Simulations of deteriorated HPC airfoils

Turbines

- Bammert and Sandstede, 1976: Effects of tolerances and blade surface-roughness on performance
- Marcu et al., 2002: Effects on unsteady loads for the MD-XX Advanced Upper Stage Engine
- Andersson et al. 2007: Effects on supersonic turbine performance
- Buske et al., 2016: MDO of a turbine blade considering casting variability

A *Non-Proprietary* Platform for Investigating Unsteady Aero and Heat Transfer

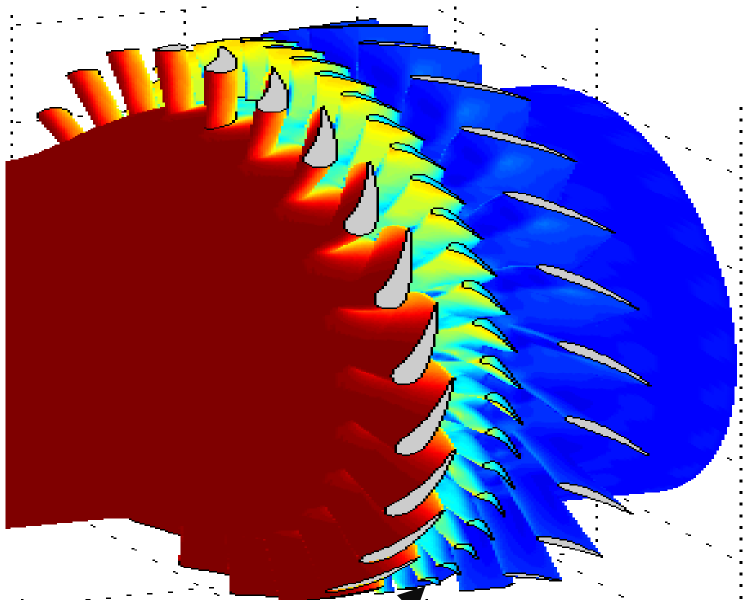

Designed to a Gov't Study Cycle of Interest :

Pressure Ratio	3.75 (total-total)		
Reaction	49.5% (static pressure)		
AN^2 (m^2 rpm^2)	37.0 $\times10^6$ (Engine)		
	1V	1B	2V
Turning	77°	116°	11°
M_{exit}	0.88	1.30	0.89
Airfoil Count	23	46	23
Zweifel Coefficient	0.83	1.05	0.40

1B

947 Sensors to Measure Heat Transfer and Unsteady Pressure

Unsteadiness Due to Downstream Interaction is Dominated by First Harmonic of Vane Passing

1B Suction Side, Power-Spectral Densities

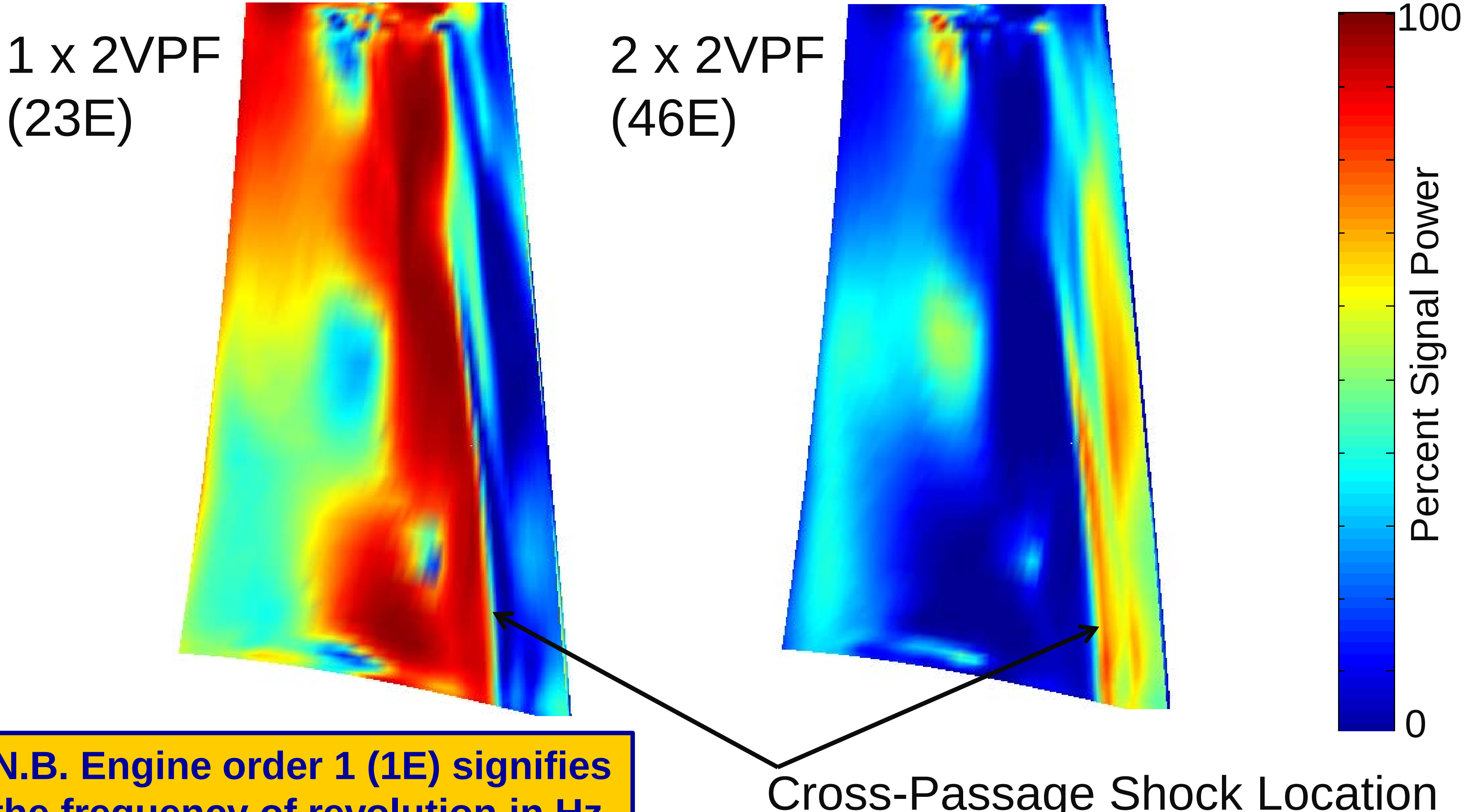

N.B. Engine order 1 (1E) signifies the frequency of revolution in Hz.

Careful Analysis of Turbine Flowfield Reveals the Source of 46E Unsteadiness

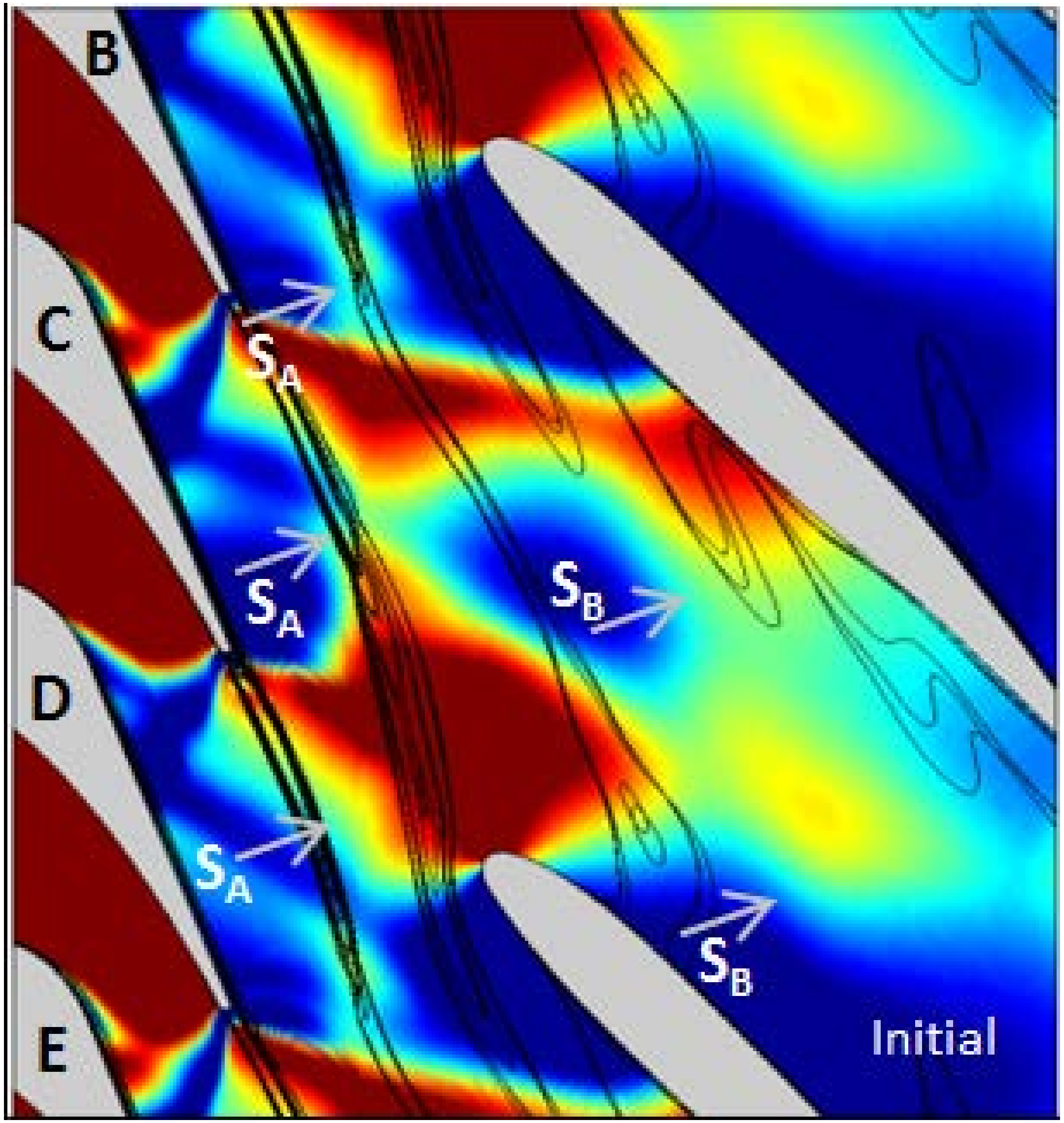

Reflected shocks are labeled with subscripts indicating originating blade, e.g.

- S_A traveling upstream toward blades
- S_B impinging on 2V PS and reflecting to neighboring SS

Each blade is impacted by shocks from the second and third preceding blades, e.g.

- Blade D impacted by shocks from blades A and B

Note: Shocks become more aligned with circumferential direction with travel upstream

Approved for Public Release (88ABW-2017-5138)

Blade Predicted and Measured Unsteadiness Spectra

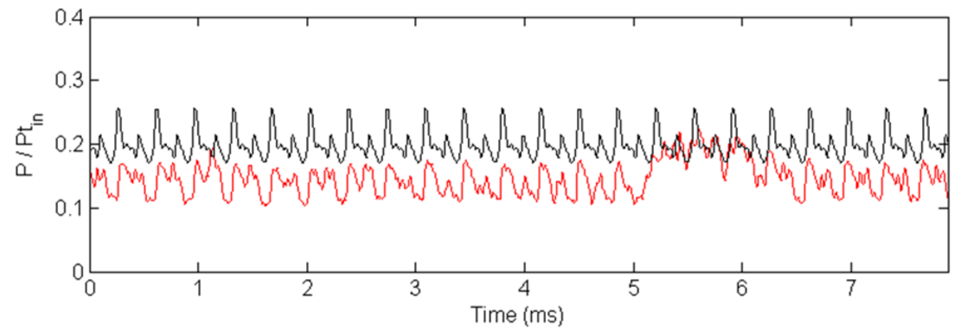

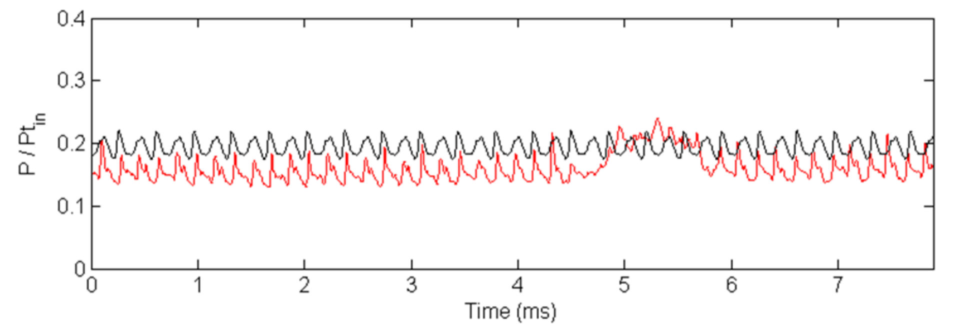

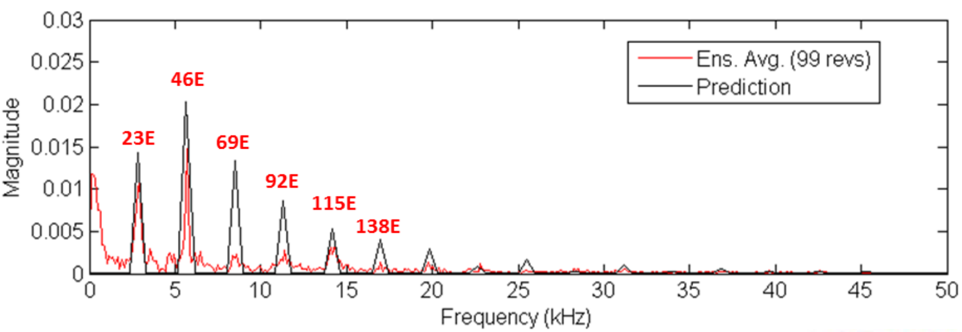

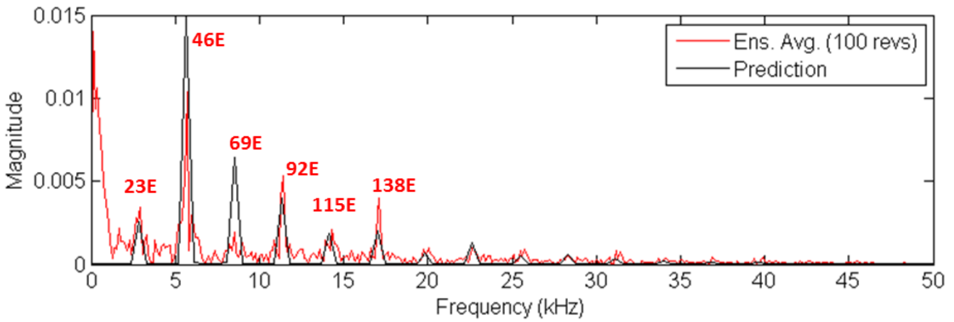

Experimental and Predicted DFT of PRZA14 (Blade SS, 15% Span, 87.7% Axial Chord)

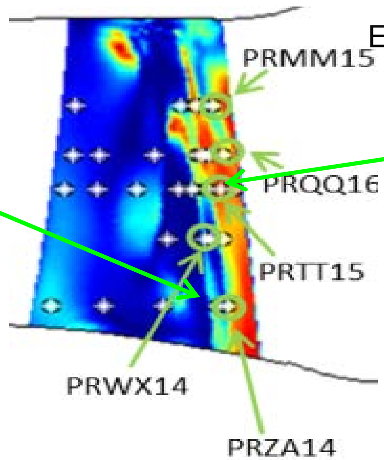

Experimental and Predicted DFT of PRTT15 (Blade SS, 49.5% Span, 88.1% Axial Chord)

	Predicted DFT Mag. Deviation (kPa)			
	23E	46E	69E	92E
15% Span 87.7% Chord	1.14	2.13	4.23	2.27
49.5% Span 88.1% Chord	-0.34	1.78	1.74	-0.51

Blade Optical Scans

- 105 airfoils produced by PCC were available for optical scanning:
  - 46 airfoils in test turbine (includes final machined surfaces and cooling holes on 37 of 46 airfoils)
  - 59 spares (raw castings)
  - All measured airfoils are available for further analysis
- Airfoils measured via blue structured-light optical scanner
  - 8 megapixels
  - 50.8 μm (2 mil) resolution
  - Repeatable accuracy of 7.62 μm (0.3 mil).
  - Dovetails and/or platforms were used for alignment

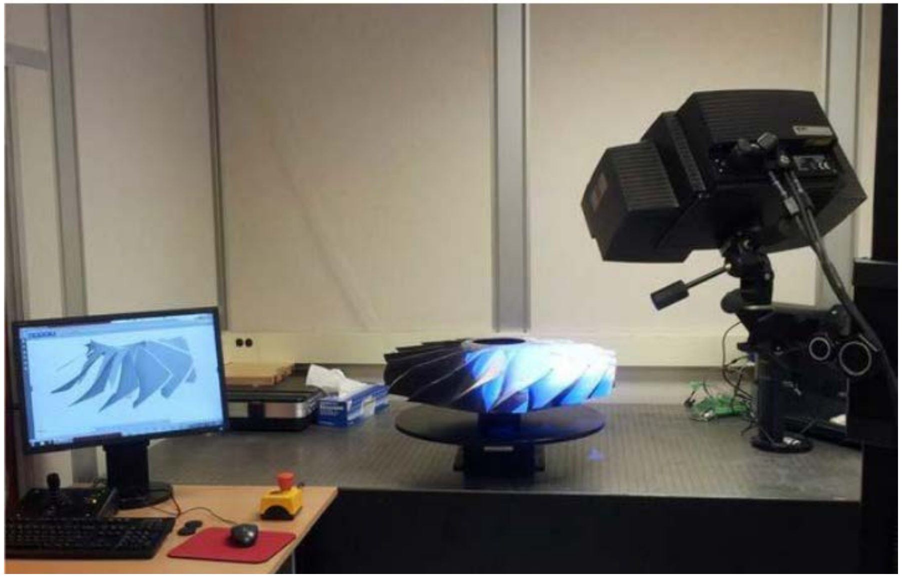

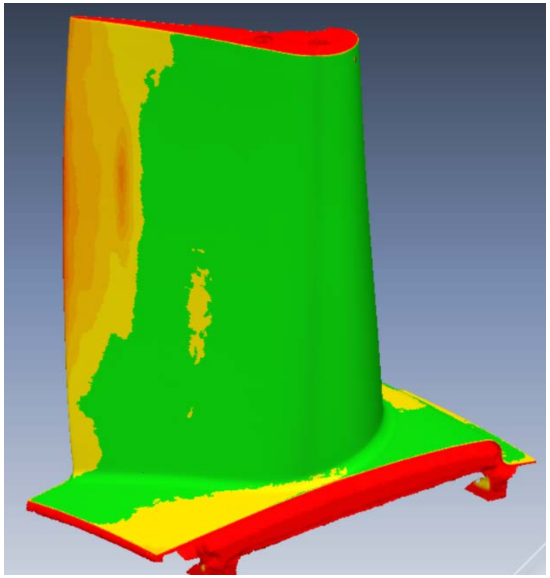

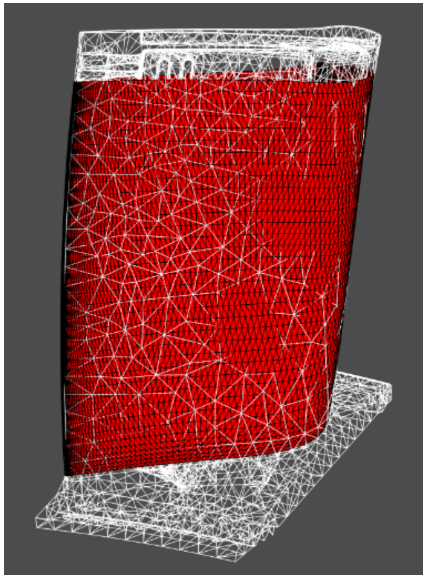

Approved for Public Release (88ABW-2017-5138)

Substantial Variation in the Cast Geometry Exists from Blade-to-Blade

Mean variation from nominal for 105 measured airfoils :

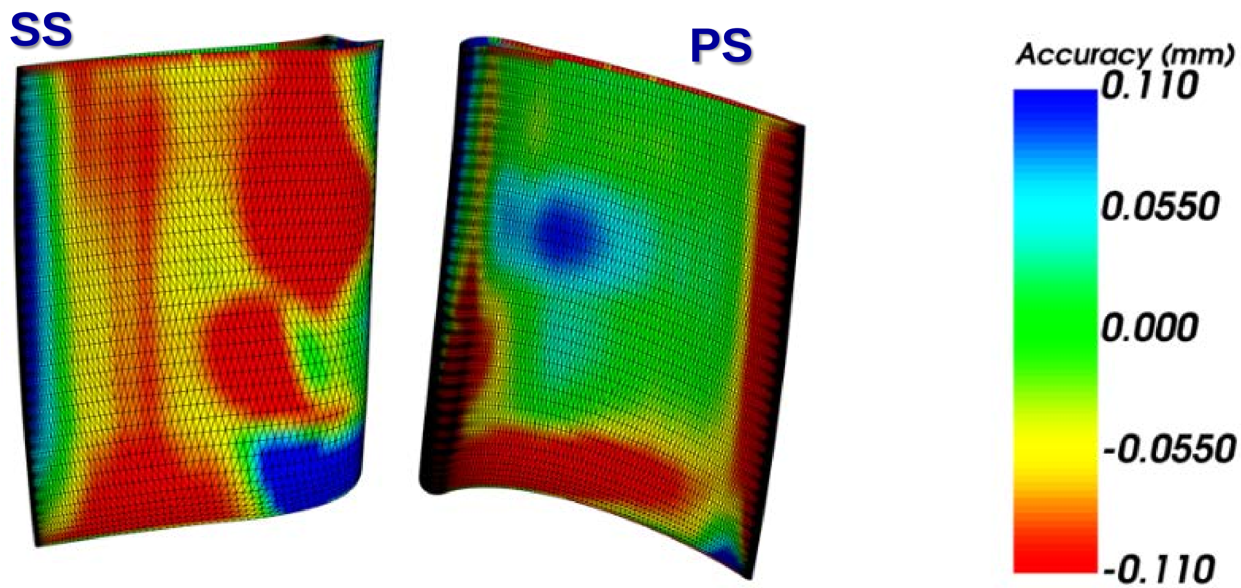

Standard deviation from nominal for 105 measured airfoils :

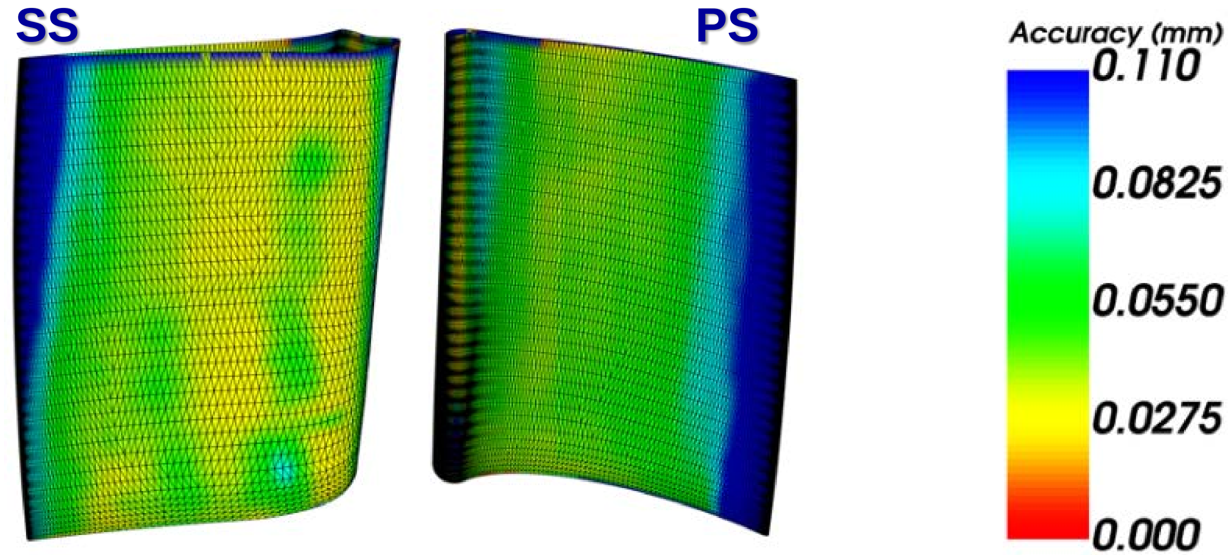

AFRL Design Tools Utilize the HuberFoil Algorithm for Airfoil Parameterization

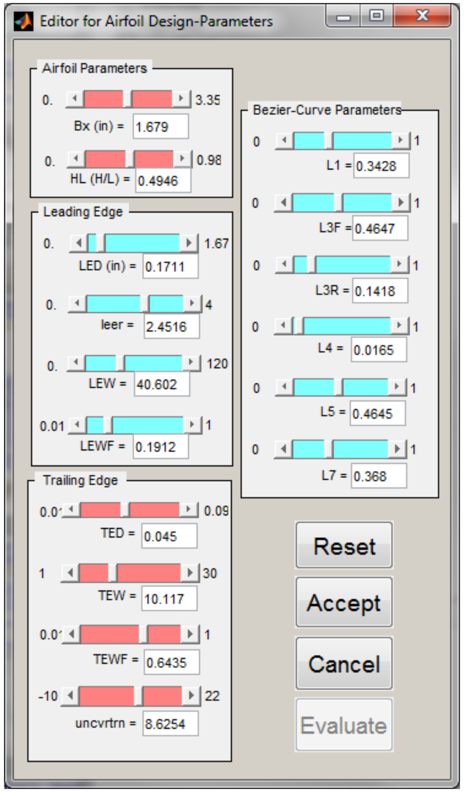

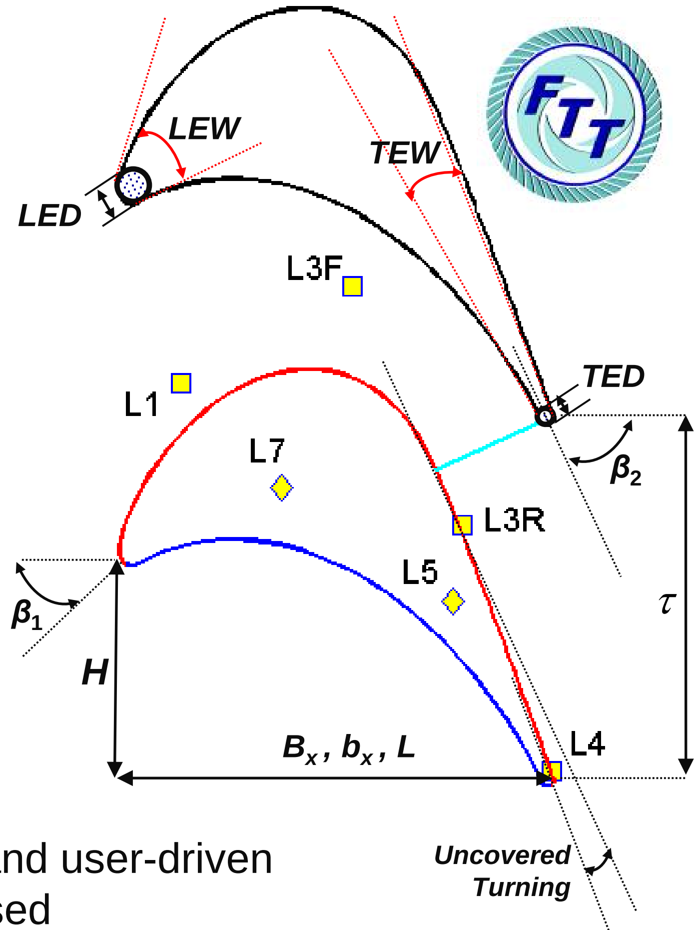

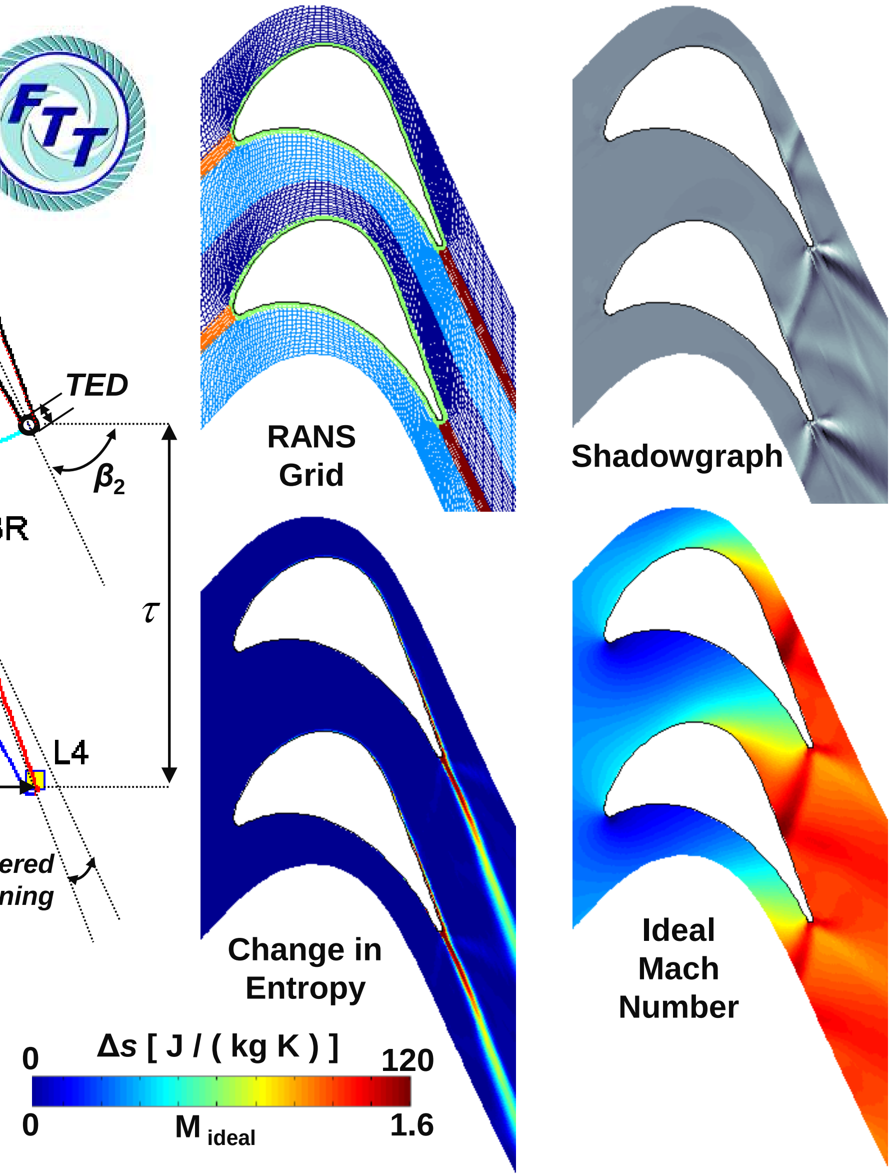

- Design optimization and user-driven shape iteration are used
- 2-Equation RANS analysis using code LEO is used for profile design
- GUI-based flowfield and grid interrogation are available

Variation in Trailing-Edge Parameters That Likely Affect 1B-2V Interaction

1B Midspan Geometry

	As-Measured		*Nominal*
	Mean	**Standard Deviation**	
Diameter (mm)	**1.033**	**0.206**	**1.138**
Wedge Angles (rad)	**0.1166**	**0.0361**	**0.1073**
Metal Angles (rad)	**1.1207**	**0.0191**	**1.1462**

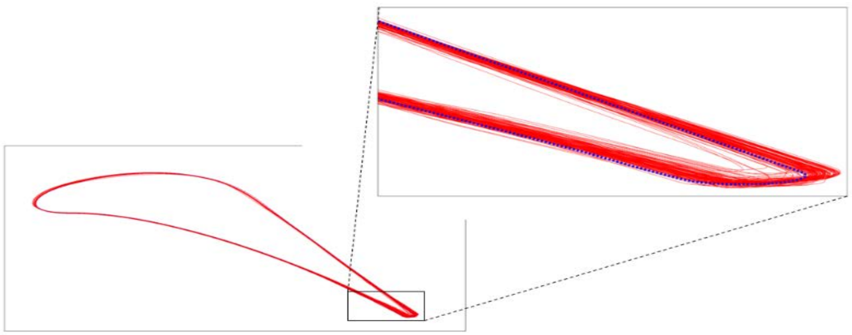

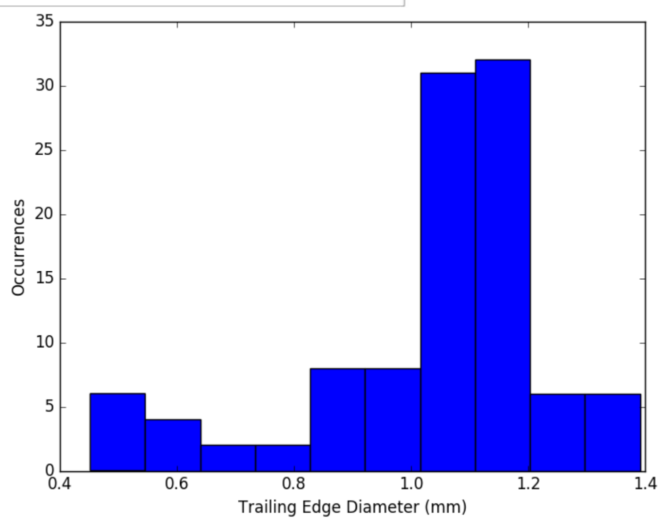

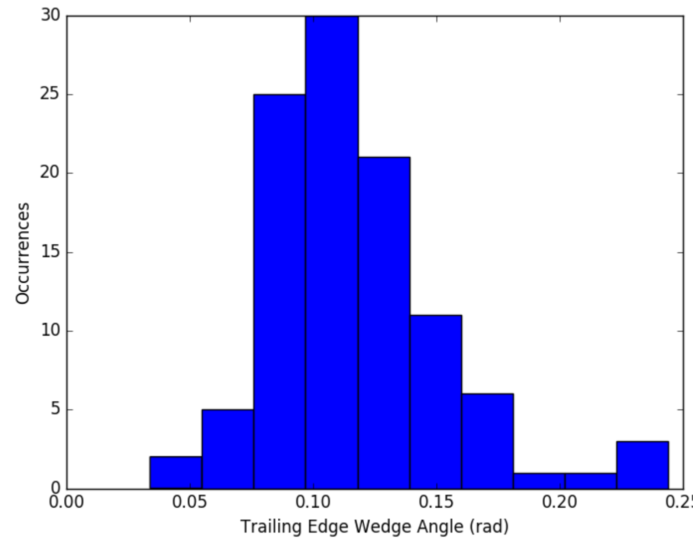

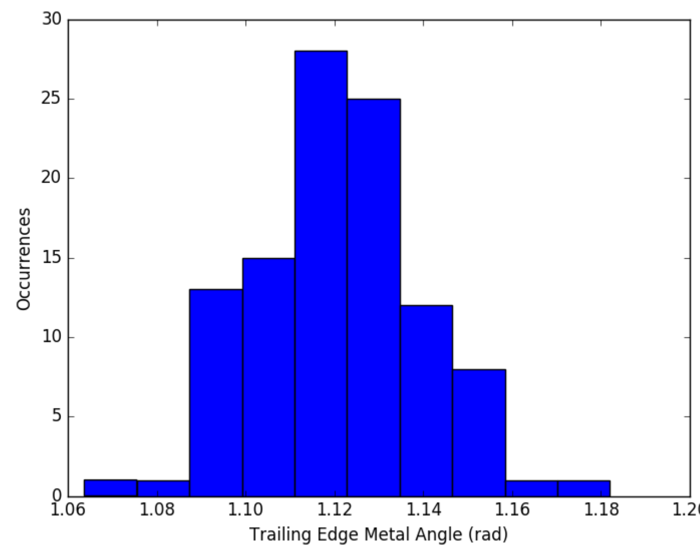

Simulation Details for This Study

Case Setup :

- Steady simulations run to 8000 iterations
- Approximately 5.3M nodes per 1/2/1 sector provided sufficient spatial resolution
- 400 time-steps per cycle (or a time-step of 0.883 μs) gave sufficient temporal resolution
- 15 cycles to periodic convergence
- 2 post-processing cycles

Cases Executed :

- 105 1/2/1 sector models with each measured blade run independently
- Full-wheel with 46 measured blades in as-built configuration
- 2/4/2 sector model with blades 20-23
- Reduced unsteadiness 2/4/2 sector model

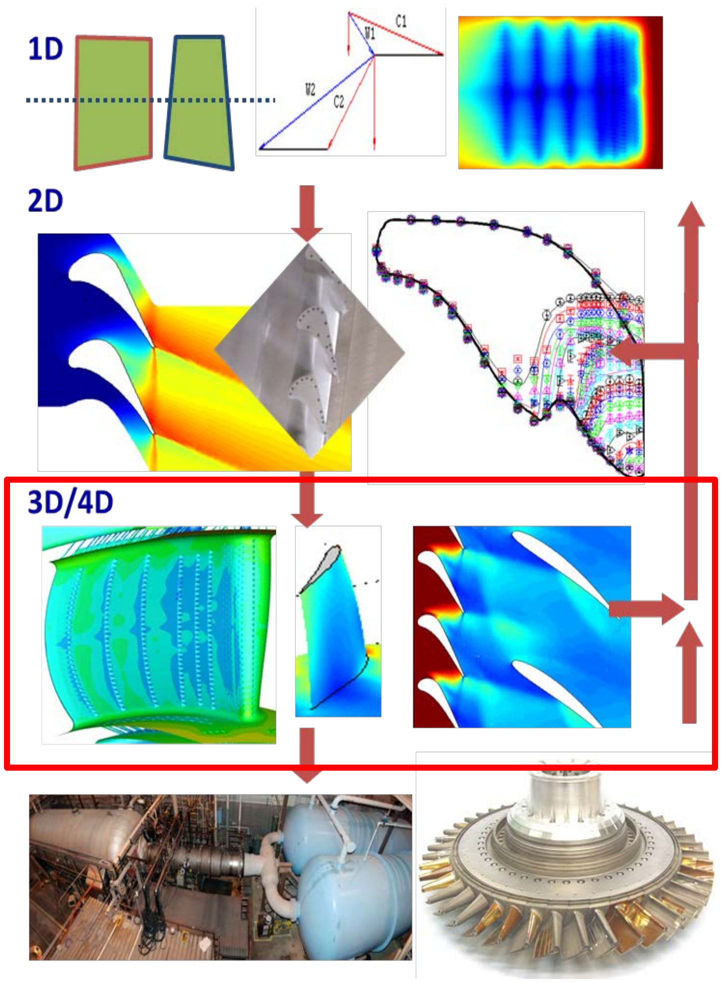

CFD Mesh Morphing

- MORPH algorithm used to alter the as-designed “blueprint” unsteady CFD mesh to fit the scanned airfoil surfaces
- New approach to generating as-manufactured CFD meshes
  - Uses full, dense, unstructured surfaces meshes
  - Collected with structured light scanning systems
  - Uses machine learning algorithms
  - Some small modifications required to ignore cooling holes and instrumentation cutouts

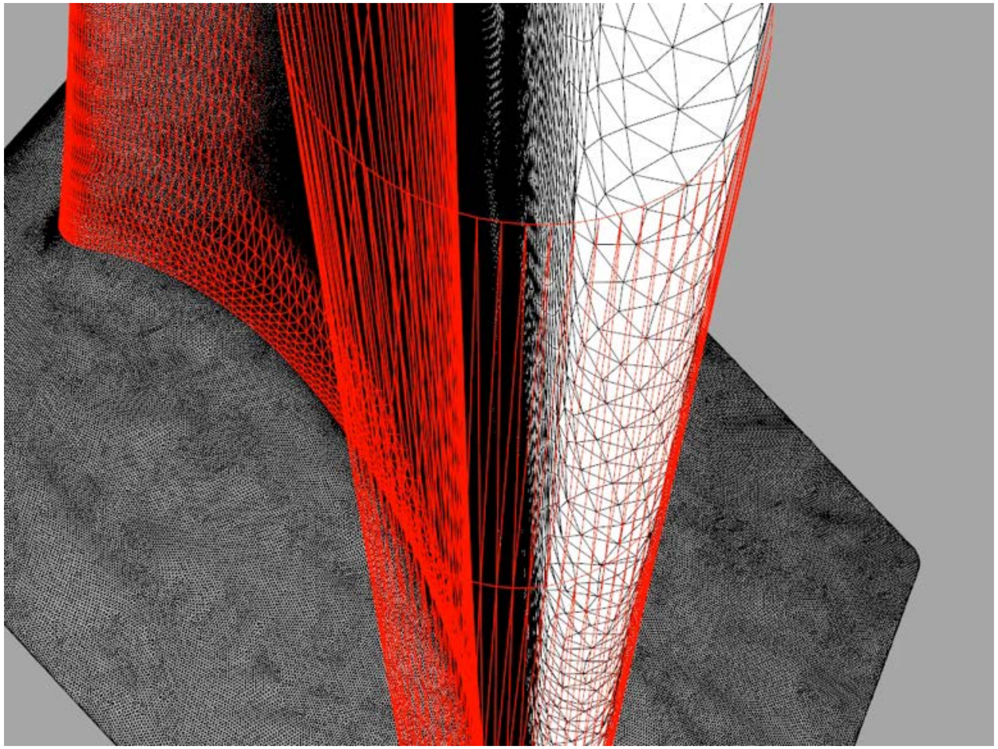

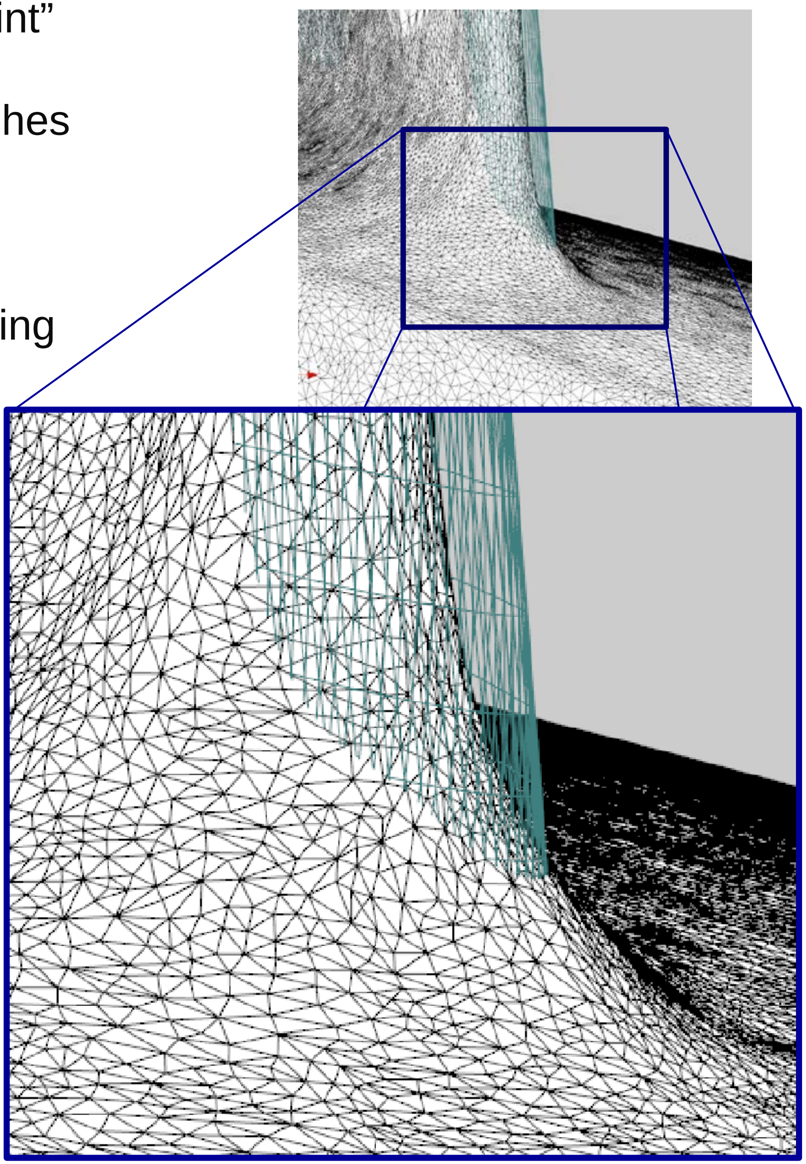

Approved for Public Release (88ABW-2017-5138)

Numerical Method in Code Leo

- Basic Flow Solver
  - Density-based code
  - Finite volume approximation to each element
    - Green's theorem applied to find partial derivatives
      - $\Delta U / \Delta X = \Sigma (U_a \, Area_x) / Volume_e$
    - Distribution formula used to obtain
      - Second derivatives
      - Upwind biased due to convection and propagation
    - Four types of element covered
      - Tets pyramid, prism, and hex
  - Explicit time-marching scheme
  - Blend of 2nd and 4th order smoothing used to reduce oscillation of the flow field due to shocks and transient

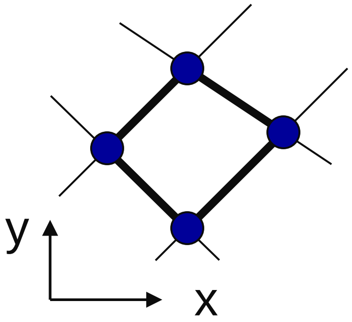

- Convergence acceleration schemes
  - Multi-grid scheme → structured mesh
  - Residual propagation method → unstructured mesh

- Dual time-stepping method for time resolve flow simulations
- Preconditioning applied to speed up convergence for low speed flow problems
- Heat conduction module employs same numerical method
- Shock capturing technique
  - 2nd order smoothing to stabilize overshoots
  - Pressure gradients used to determine where to apply smoothing

RANS Models of the Turbine Were Developed Carefully

- Iterative Convergence
  - Executing steady state simulations until residuals are sufficiently small [1]
- Grid Convergence
  - Determining sufficient grid spatial resolution to capture flow physics [1,2]
- Temporal Convergence
  - Determining the minimum temporal resolution required to capture flow physics [1]
- Periodic Convergence
  - Executing time-accurate solution until the true periodic nature of the flowfield is obtained [3]
- Geometric Model Convergence
  - Finding the minimum wheel sector required to represent the full annulus

[1] AIAA, 1988 , "Guide for the Verification and Validation of Computational Fluid Dynamics Simulations," AIAA G-077-1998.

[2] Roache, P. J., 1997, "Quantification of Uncertainty in Computational Fluid Dynamics," *Annual Review of Fluid Mechanics*, Annual Reviews, Inc., Palo Alto, CA, pp. 126-160.

[3] Clark, J. P., and Grover, E. A., 2007, "Assessing Convergence in Predictions of Periodic-Unsteady Flowfields," ASME *Journal of Turbomachinery*, Vol. 129, pp. 740-749.

Geometric Model Convergence

DFT Magnitude at 46E (5.84kHz)

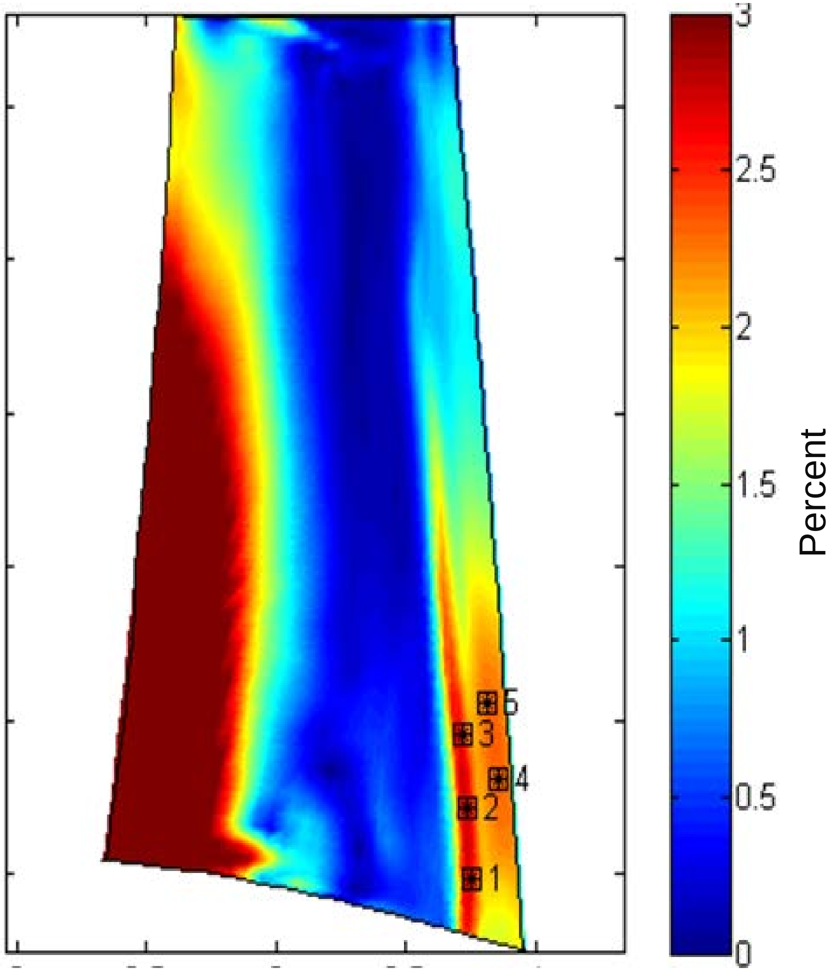

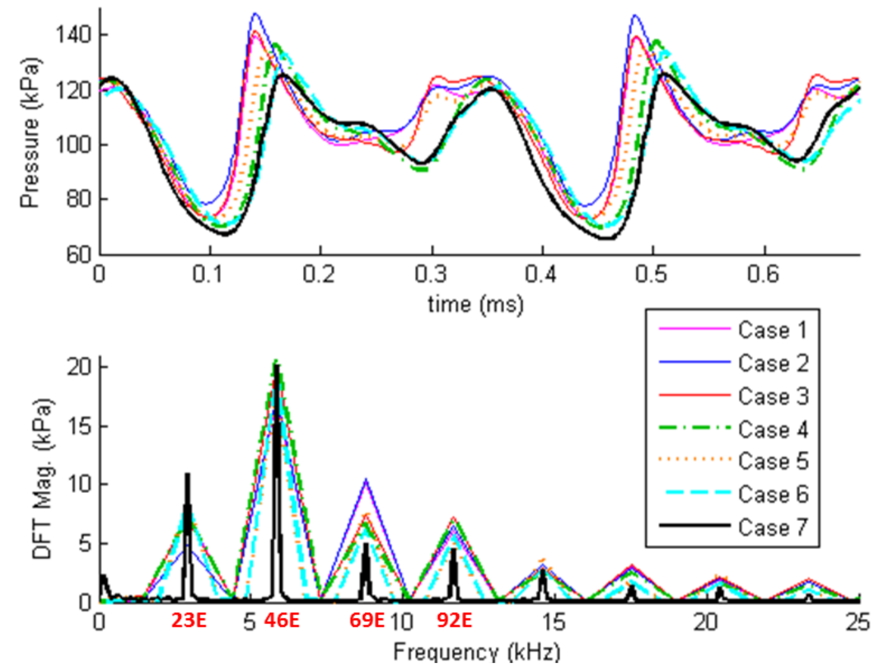

	Maximum Static Pressure Difference (Percent)					
	Case 1	Case 2	Case 3	Case 4	Case 5	Case 6
Point 1	10.81	17.07	10.87	9.39	7.30	6.64
Point 2	4.94	9.59	3.94	2.93	5.35	2.42
Point 3	4.44	6.89	6.48	1.51	2.09	0.37
Point 4	10.60	13.03	13.51	2.67	11.84	1.43
Point 5	17.41	13.98	16.33	4.81	13.44	9.27

Geometric Model Convergence

Case 6 (3c 1V, 4c/2u 1B, 3u 2V) determined to have sufficiently modeled the HIT RT.

- Pressure traces at 5 point in areas of highest unsteadiness tracked closely to full-wheel simulation
- Downstream suction-side surface aft of cross-passage shock of case 6 compares well with full-wheel analysis

	Case 1	Case 2	Case 3	Case 4	Case 5	Case 6
Average Deviation (%)	5.09	3.80	5.08	3.46	2.98	1.80
Maximum Deviation (%)	11.90	11.11	10.06	9.77	6.59	5.57

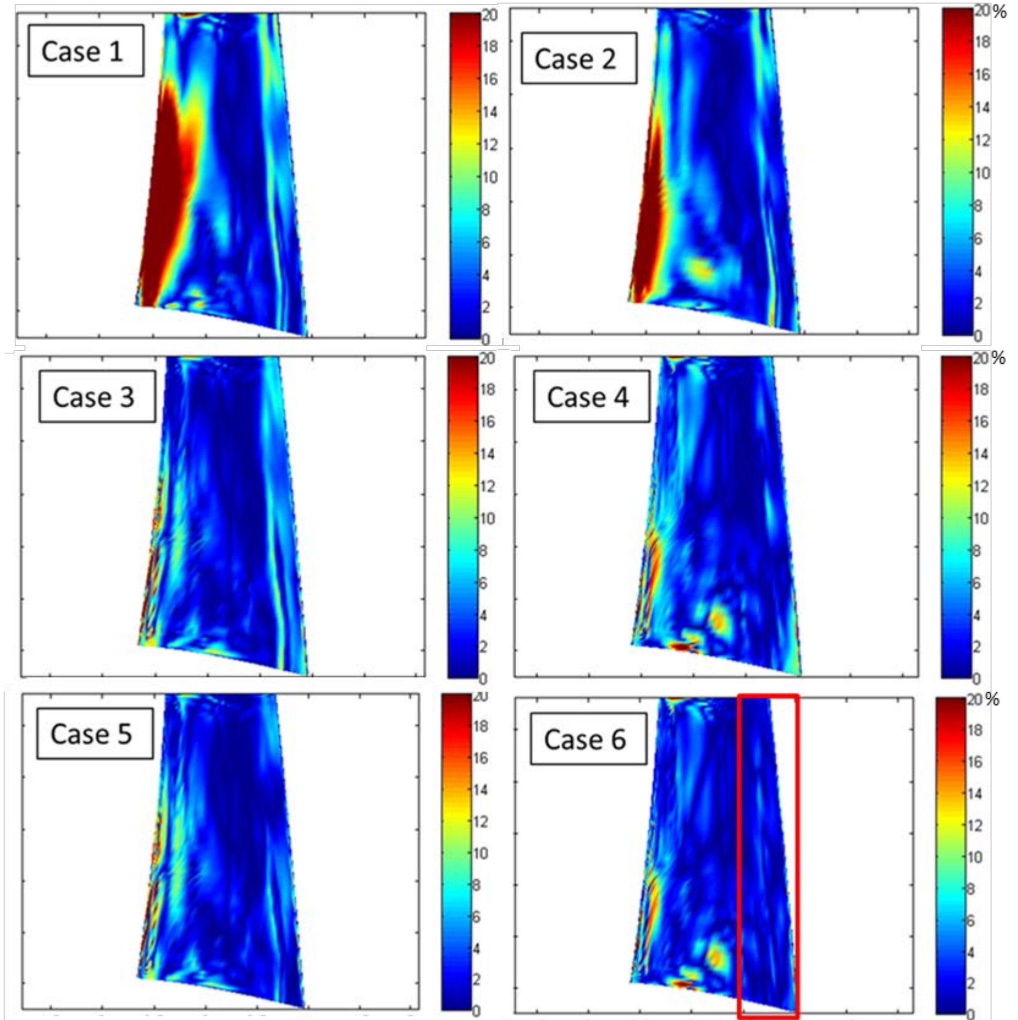

Differences of the Normalized DFT Magnitudes at 46E of the Full-Wheel Simulation and Each Sector as a Percentage of the Maximum Unsteadiness of the Full-Wheel Simulation

Unsteadiness Due to Shock Reflections Varies Markedly from Blade-to-Blade

46E Unsteadiness

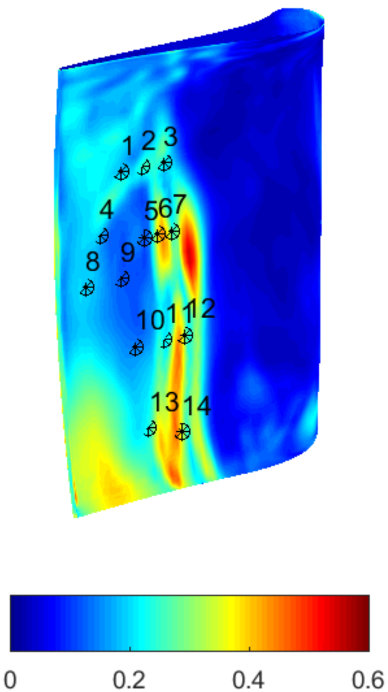

100 (Standard Deviation of DFT mag.) / Ptin

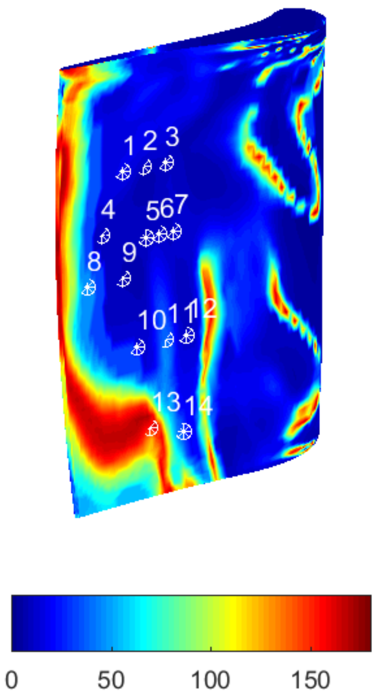

Standard Deviation of DFT Phase Angle (degrees)

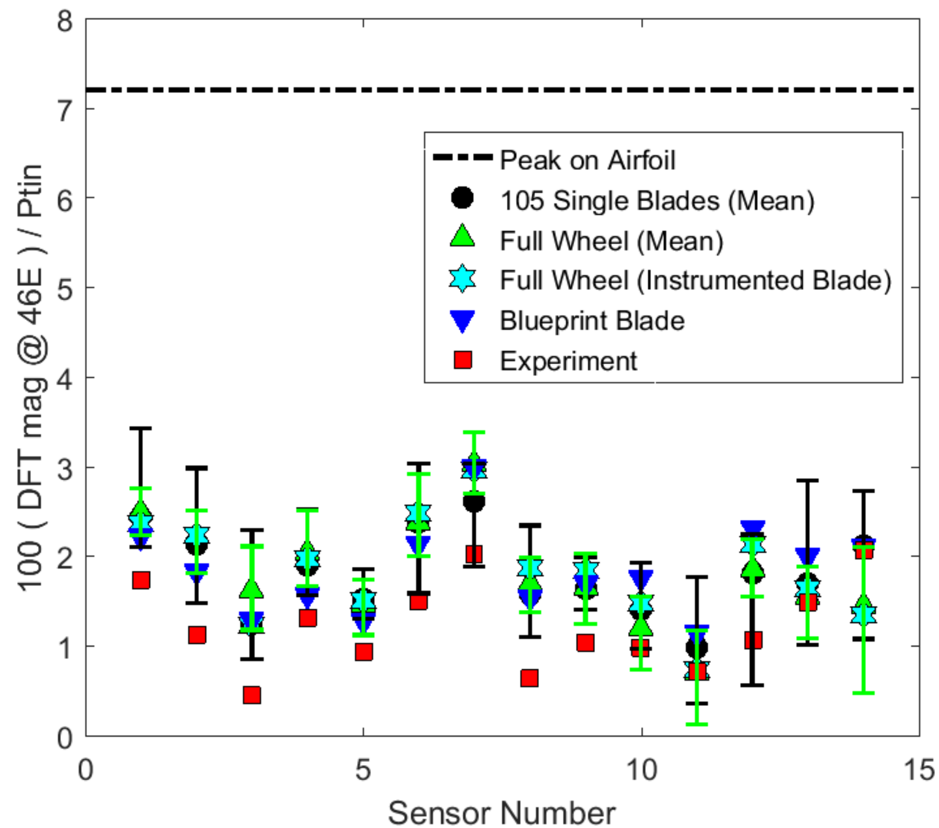

It Should be Possible to Reduce the Unsteadiness on a Blade of Interest

Consider Sensor #7 at Blade 20 (G3VFH)

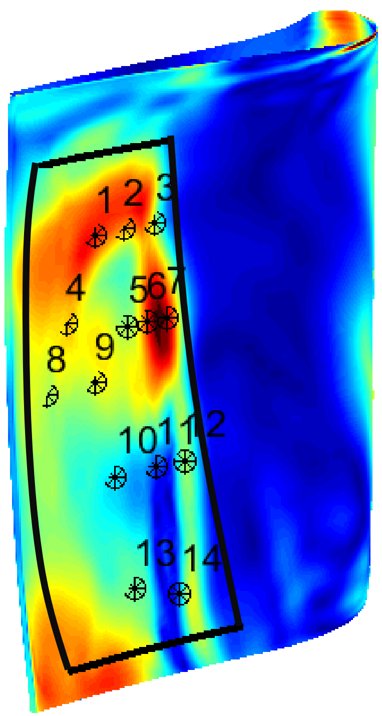

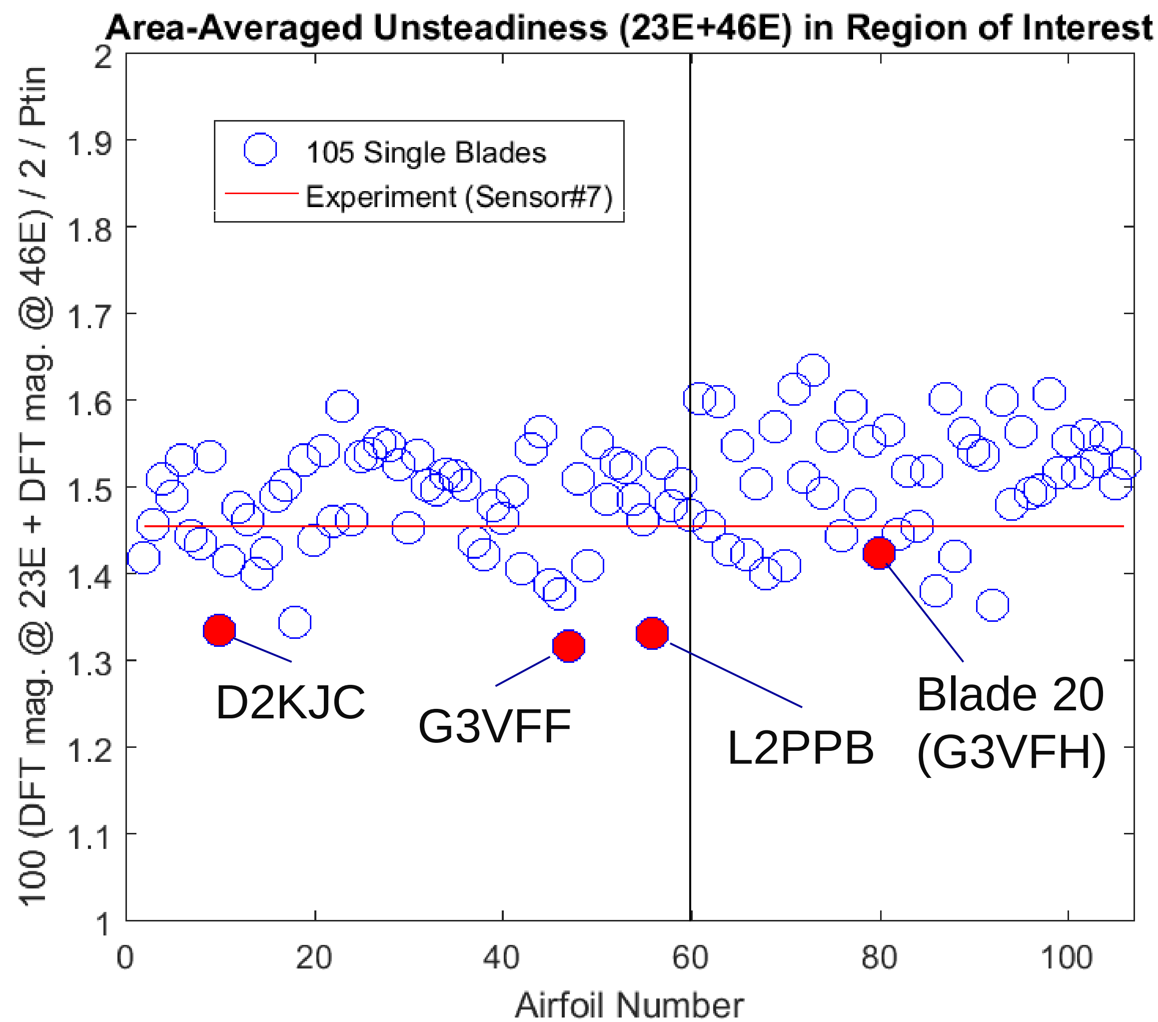

Again, Consider the Source of 46E Unsteadiness

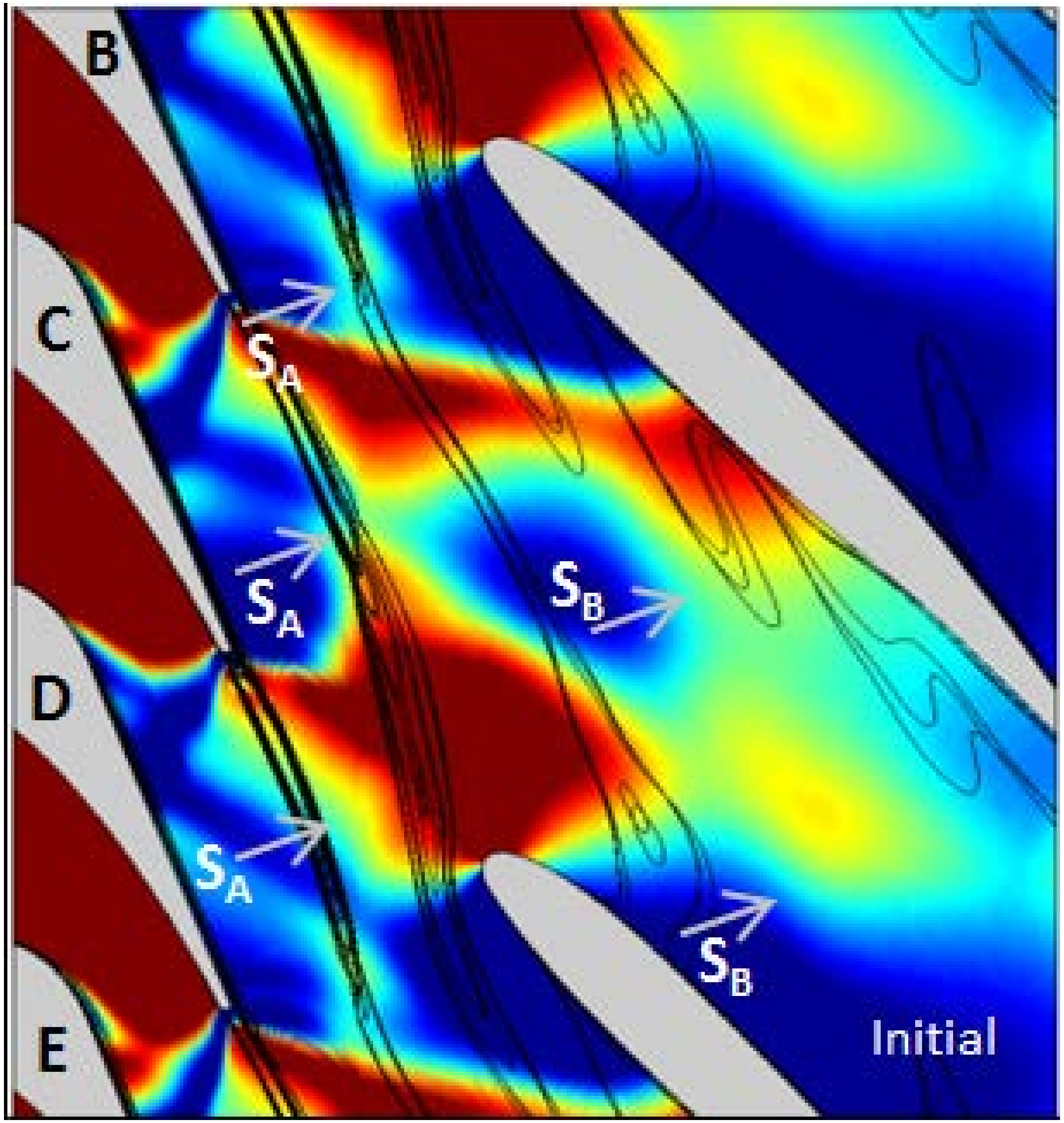

Reflected shocks are labeled with subscripts indicating originating blade, e.g.

- S_A traveling upstream toward blades
- S_B impinging on 2V PS and reflecting to neighboring SS

Each blade is impacted by shocks from the second and third preceding blades, e.g.

- Blade D impacted by shocks from blades A and B

Note: Shocks become more aligned with circumferential direction with travel upstream

Previous Analysis Indicated that Shocks Impact 1B from 2 and 3 Passages Away

Unsteadiness on Blade 20 : Full-Wheel Calculation

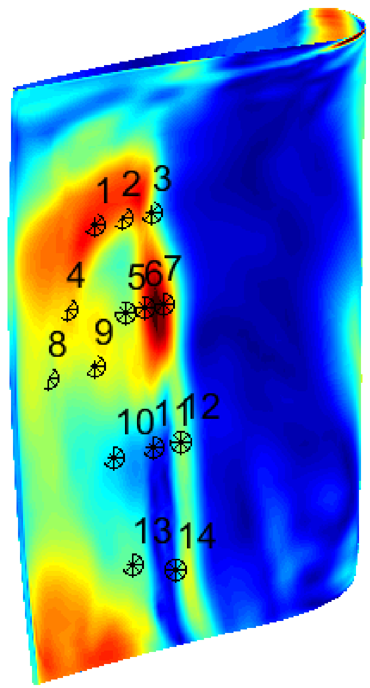

Unsteadiness on Blade 20 : 2/4/2 Model : Blades 20-23

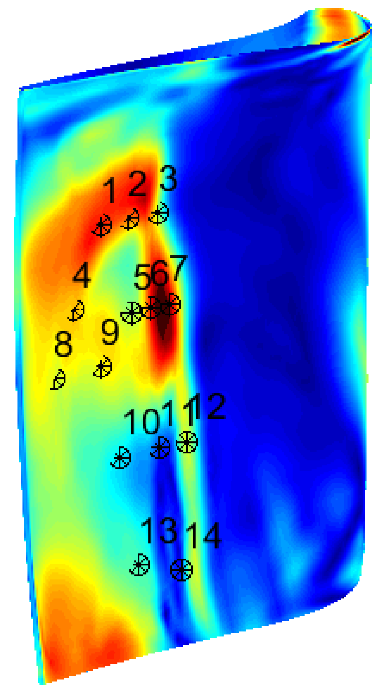

100 DFT mag. / Pt_{inlet} @ 46E

Unsteadiness at Blade 20, Sensor #7 is Substantially Reduced from Initial Level

Full-Wheel Calculation

2/4/2 Model with Blades D2KJC, L2PPB, and G3VFF at positions 21-23.

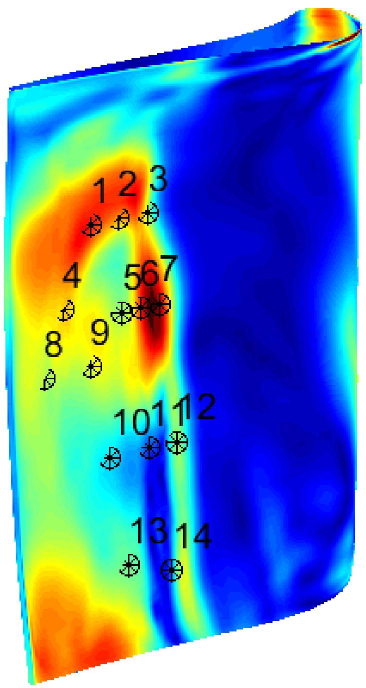

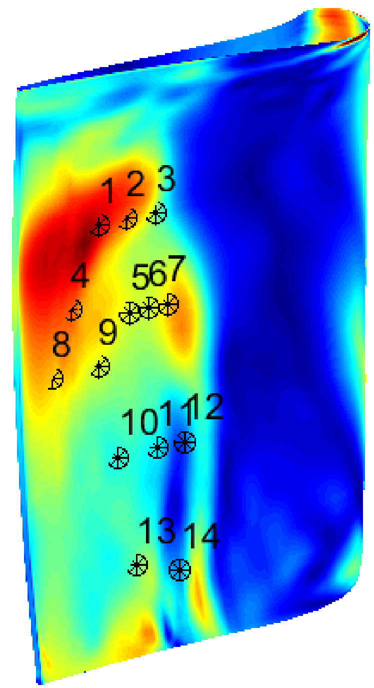

100 DFT mag. / Pt_{inlet} @ 46E

Blade-to-Blade Performance Data

- “Rig efficiency” : Aeroperformance was calculated from mixed-out average quantities between rig inlet- and exit-rake locations

- 105 1/2/1 sector models with each measured blade run independently :

  Delta efficiency from nominal (i.e. blueprint) result :

  Minimum = -0.4%
  Maximum = 0.6%
  Standard deviation = 0.2%

- Full-wheel with 46 measured blades in as-built configuration :

  Delta efficiency from nominal (i.e. blueprint) result = -0.1%

Wavelet Scalograms Reveal Blade-to-Blade Variations on 2V Sensors

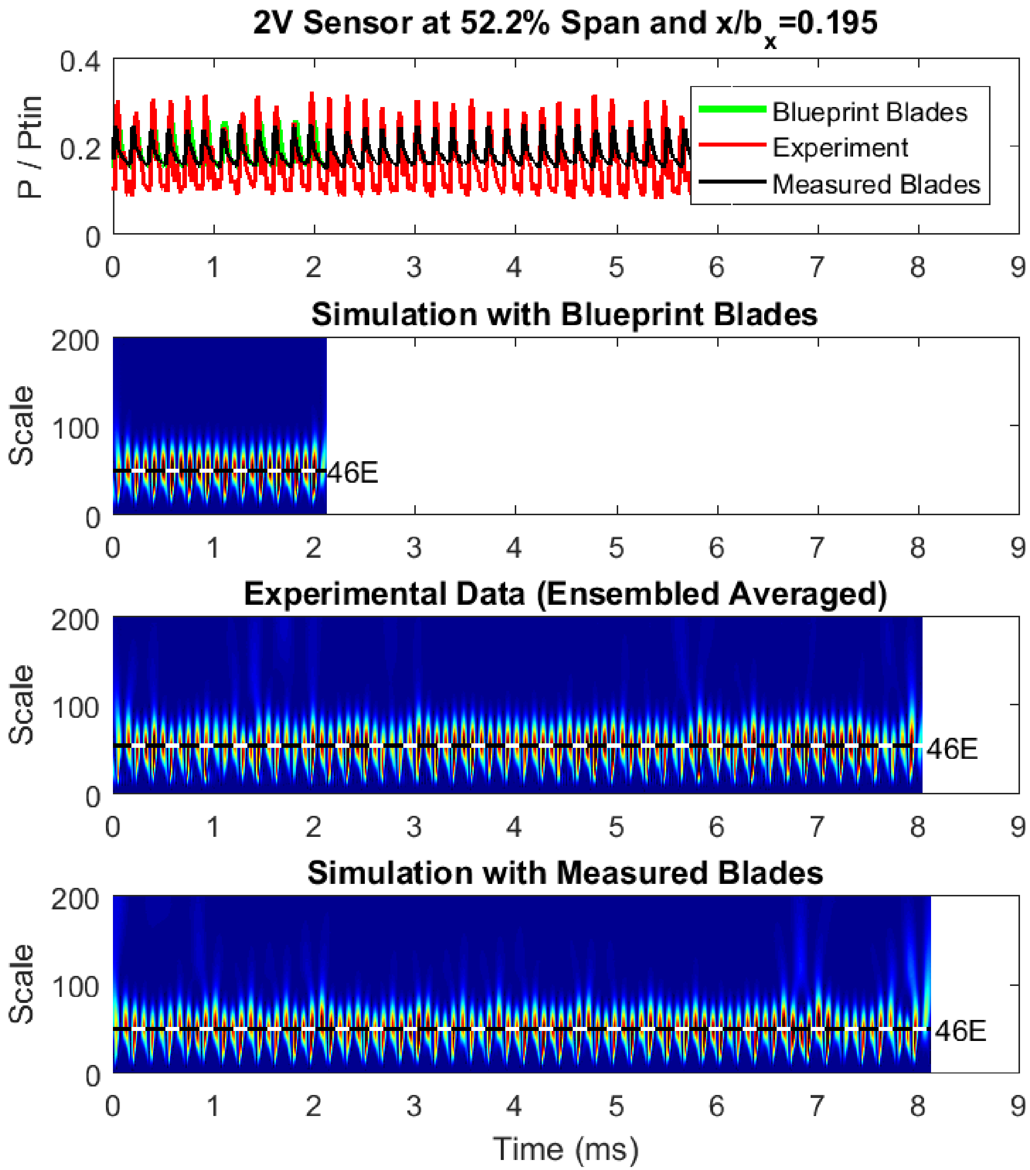

There are Also Vane-to-Vane Variations Apparent in the Data (Not Modeled)

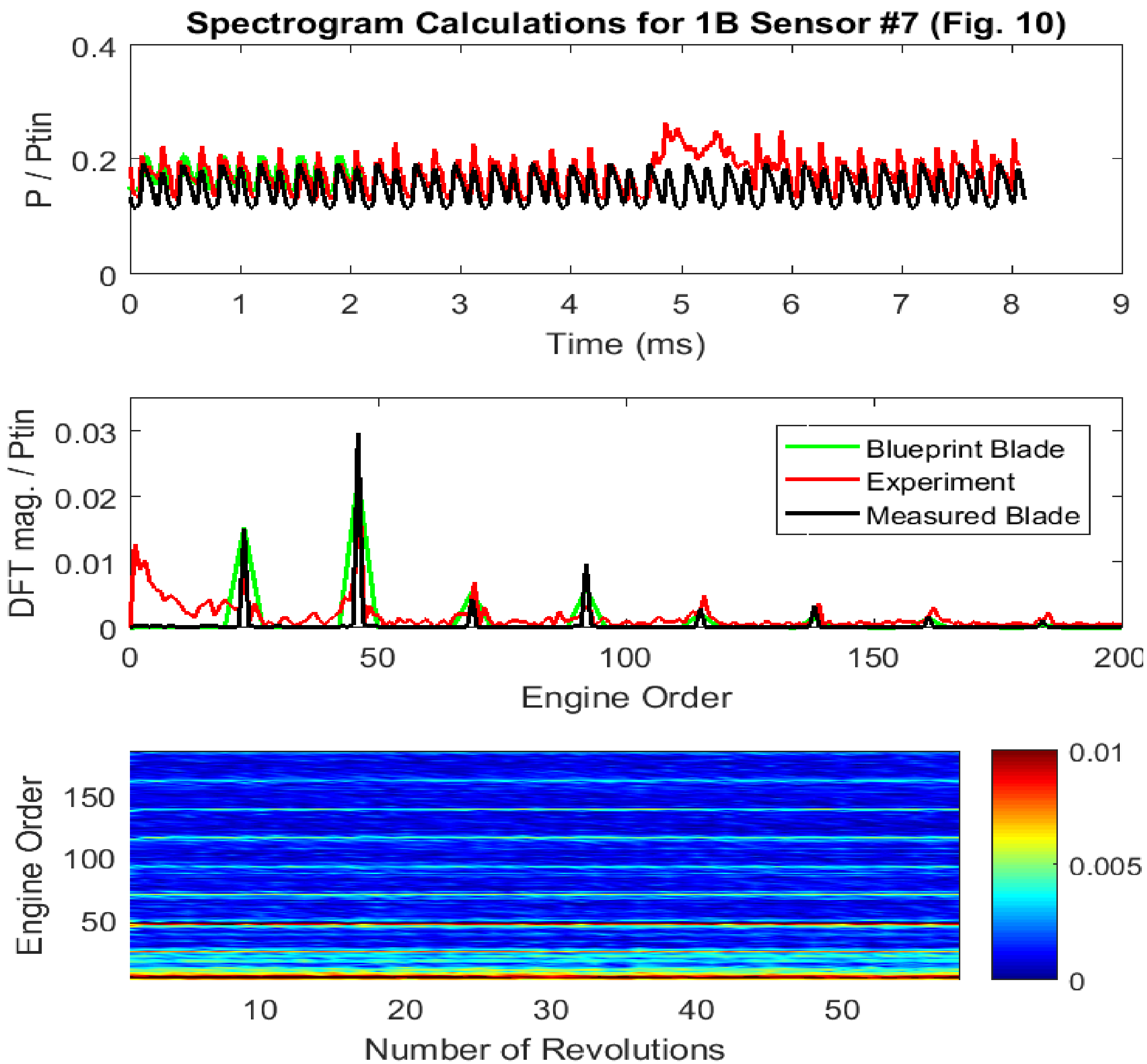

Summary and Conclusions

- The effect of as-manufactured geometry variations on unsteadiness due to shock reflections in a transonic turbine was assessed.
- 105 individual blades were simulated as well as the as-built full wheel.
- Substantial blade-to-blade variations were observed.
- For blades that are expected to have high resonant stress or where small performance improvements are the goal, a final design prediction with measured geometries is warranted.
- The availability of predicted flowfields for measured airfoils made it possible to reduce the unsteadiness on a target blade.